Electrochemistry Communications 50 (2015) 24–27

Contents lists available at ScienceDirect

Electrochemistry Communications

journal homepage: www.elsevier.com/locate/elecom

Short communication

A Ni_3S_2-PEDOT monolithic electrode for sodium batteries

Chaoqun Shang [a,b,1], Shanmu Dong [a,1], Shengliang Zhang [a,b], Pu Hu [a,b], Chuanjian Zhang [a], Guanglei Cui [a,*]

[a] Qingdao Industrial Energy Storage Research Institute, Qingdao Institute of Bioenergy and Bioprocess Technology, Chinese Academy of Sciences, No. 189 Songling Road, 266101 Qingdao, China
[b] University of Chinese Academy of Sciences, Beijing 100049, China

ARTICLE INFO

Article history:
Received 11 October 2014
Received in revised form 1 November 2014
Accepted 2 November 2014
Available online 10 November 2014

Keywords:
Sodium batteries
Ni_3S_2
PEDOT
Monolithic Ni_3S_2-PEDOT electrode

ABSTRACT

Ni_3S_2 attracts much attention for sodium batteries owing to its natural abundance, low cost, and high theoretical capacity. However, poor conductivity of Ni_3S_2 and large volume expansion hamper its potential application. We describe a facile strategy to construct monolithic Ni_3S_2-Poly(3,4-ethylenedioxythiophene) (PEDOT) electrodes with stable electrochemical performance for sodium batteries. Ni_3S_2 is directly grown on Ni foam substrate with superior electron transport efficiency. The PEDOT layer would efficiently protect the Ni_3S_2 from being wrecked by the severe volume expansion during charge–discharge process. The as-prepared Ni_3S_2-PEDOT electrodes display stable cycling performance with a capacity of 280 mAh g^{-1} after 30 cycles between 0.5 and 2 V.

1. Introduction

Rechargeable Na batteries have attracted tremendous attention because of their low cost and natural abundance of sodium [1,2]. To realize Na technology, a variety of cathodes and electrodes have been explored for Na-storage capability [3–8]. As a promising electrode candidate of sodium batteries, Ni_3S_2 has many advantages including rich in natural resources, low cost, environmental friendly and high theoretical capacity [9–11]. However, the poor conductivity of Ni_3S_2 hampers its potential application [12–14]. To address this issue, designing monolithic electrodes with well electronic conductivity is a promising strategy [15]. One of the most attractive concepts is to directly grow Ni_3S_2 on electroconductive substrates as binder-free electrodes [12]. In this design, many competitive benefits such as short ion transport pathways, superior electron transport efficiency and rich accessible electroactive sites are simultaneously achieved to exhibit desirable electrochemical performance [16–18]. On the other hand, the large volume change during discharge and charge caused by the inherent large size of Na ion (35% much larger than Li ions in radius) may lead to rapid capacity fading [19]. This problem can be alleviated if an electroactive polymer layer with good binding compatibility was introduced to protect Ni_3S_2. Therefore, much attention has been paid to Poly(3,4-ethylenedioxythiophene) (PEDOT) because of its high stability, mechanical flexibility and excellent conductivity [20–22].

In this communication, we adopt a facile strategy to design monolithic Ni_3S_2-PEDOT electrode for sodium-ion batteries. Ni_3S_2 is directly grown on Ni foam substrate and the PEDOT protective layer was electrodeposited subsequently. The monolithic Ni_3S_2-PEDOT electrode displays a high reversible specific capacity of 400 mAh g^{-1} even at 600 mA g^{-1} and high initial coulombic efficiency.

2. Experimental

2.1. Hydrothermal preparation of Ni_3S_2

All the chemicals are used directly without further purification. In a typical synthesis process, 0.142 g Na_2SO_4 and 0.048 g $Na_2S_2O_3$ are dissolved into 40 mL deionized water to obtain a transparent solution. The solution is transferred into Teflon stainless steel autoclave with a piece of Ni foam (5 cm × 3 cm) in it. The autoclave is kept in an oven at 150 °C for 3 h. After cooled down to room temperature, the Ni foam in the autoclave changes into black that Ni_3S_2 is obtained. This black Ni_3S_2 is washed with deionized water and absolute ethanol for three times, then dried at 120 °C in vacuum oven for 8 h. The active Ni_3S_2 is about 1 mg cm^{-2} on Ni foam, which is calculated from $m(Ni_3S_2) = \Delta m \times M_{Ni3S2}/2M_S$. Δm is the mass difference of Ni foam before and after hydrothermal synthesis ($3Ni \rightarrow Ni_3S_2$). The mass is carefully weighed by a microbalance with an accuracy of 0.01 mg.

2.2. Electrodeposition of PEDOT on Ni_3S_2

PEDOT is synthesized at 1 V for 60 s in 40 mL aqueous solution that contained 0.45 g EDOT (3,4-ethoxylene dioxy thiophene), 0.426 g $LiClO_4$ as well as 1.6 g SDS (sodium dodecyl sulfate), where potentials are measured relative to an Ag/AgCl reference electrode using a Pt foil as a counter electrode and Ni&Ni_3S_2 as a working electrode. After electrodeposition, monolithic Ni_3S_2-PEDOT electrode is finally obtained. PEDOT is

* Corresponding author. Tel.: +86 532 80662746; fax: +86 532 80662744.
E-mail address: cuigl@qibebt.ac.cn (G. Cui).
[1] These authors contributed equally to this work.

http://dx.doi.org/10.1016/j.elecom.2014.11.001
1388-2481/

about 0.1 mg cm^{-2} after comparing the mass of electrode before and after electrodeposition, which is about 10% of active Ni_3S_2.

2.3. Characterization

XRD patterns were recorded with a Bruker-AXS Microdiffractometer (D8 Advance) using Cu Ka radiation (λ = 1.5406 Å) from 5 to 90° at a scanning speed of 3° min^{-1}. Morphological information and Energy Dispersive X-ray Spectroscopy (EDX) elemental analysis were attained from field emission scanning electron microscopy (FESEM, HITACHI S-4800).

The sodium coin cells are assembled in an argon filled glove box (<1 ppm H_2O and O_2) by using the Ni_3S_2-PEDOT as the active working electrode and sodium pieces as the counter and reference electrode, a glass-fiber and a polypropylene (Celgard 2400) as separators, and 1 M $NaClO_4$ dissolved in EC:DMC (1:1 in volume) with 10% FEC as the electrolyte. Galvanostatic charge–discharge experiments are tested in a LAND battery testing system at a current density of 600 mA g^{-1}.

3. Results and discussion

The X-ray diffraction (XRD) patterns of the as-prepared Ni_3S_2-PEDOT, Ni_3S_2 and the used Ni foam are illustrated in Fig. 1a. As can be seen, the three strongest diffraction peaks at 44.4°, 51.7° and 76.2° in all patterns are corresponding to (111), (200) and (220) of Ni (JCPDF#65-0380) framework, respectively. After hydrothermal reaction, some obvious peaks at 21.7°, 31.1°, 37.7°, 50.1° and 55.3° appear on the patterns, which can be indexed to (101), (110), (003), (113) and (112) of Ni_3S_2 (JCPDF#44-1418). No other peak suggests the high purity of the Ni_3S_2 crystalline phase we prepared. Interestingly, only the strongest peak of (110) at 31.1° can be identified after PEDOT electrodeposition of the electrode, which may indicate that PEDOT homogeneously wraps the Ni_3S_2 and further provides a flexible protective polymer layer.

Fig. 1b depicts a SEM image of the pristine Ni foam substrate, where the surface of Ni foam is smooth. As shown in the low-magnification SEM image (inset of Fig. 1b), an obvious three dimensional structure can be found. After hydrothermal treatment at 150 °C for 3 h, the surface of Ni is rough and composed of microparticles in the range of 100–400 nm (Fig. 1c). According to XRD results, these particles can be identified as Ni_3S_2. It is indicated that Ni_3S_2 is directly grown on Ni foam with fast electron path as well as good contact with electrolyte. However, owing to the large size of Na^+, the volume change during Na^+ insertion and extraction would probably destroy the integrity of Ni_3S_2 and Ni substrate, which would further impact the electrochemical performance. In order to protect Ni_3S_2 electrode, PEDOT is electrodeposited directly on Ni_3S_2 to form a flexible conductive layer. Fig. 1d displays the morphology of PEDOT protective layers, which is quite different from the morphology of Ni_3S_2. PEDOT is mostly like nanoflakes (inset of Fig. 1d). This protective layer can be expected to effectively alleviate the structure destruction of Ni_3S_2 during charge–discharge. According to EDX analysis (as shown in Table 1), the main element was Ni for both Ni_3S_2 and Ni_3S_2-PEDOT electrodes owing to the Ni foam substrate. After electrodeposition, the contents of S and O increase because of the formation of PEDOT.

The monolithic Ni_3S_2-PEDOT on Ni foam is directly explored as an õintegrated electrode for sodium batteries. Ni_3S_2 on Ni foam without PEDOT protection is also introduced as a fair comparison. Fig. 2a exhibits the initial five galvanostatic charge–discharge voltage profiles, between 0.5 and 2.8 V, of monolithic Ni_3S_2 electrode at a current density of 600 mA g^{-1}. The discharge profile can be attributed to the reaction of Na^+ and Ni_3S_2. The reversible charge capacity of Ni_3S_2 is about 78%, which may be caused by the large volume change and irreversible side reactions. On the other hand, Ni_3S_2 electrode delivers poor cycle stability that there is only 60% capacity retention after five cycles. The effect of PEDOT protective layer to buffer the volume change is apparent, where Ni_3S_2-PEDOT electrodes display high coulombic efficiency and stable cycle performance as shown in Fig. 2b. Fig. 2e shows the change in XRD patterns of the Ni_3S_2-PEDOT electrode during the initial electrochemical discharge and charge reaction. After the first discharge reaction, the peaks of Ni_3S_2 (110) disappear with new peaks of Na_2S occurring. It is suggested that Ni_3S_2 changes into Na_2S and Ni ($4Na^+ + 4e^- + Ni_3S_2 \rightarrow 3Ni + 2Na_2S$). While being charged at 2.8 V, the peaks of Ni_3S_2 (110) appear with decreased intensity compared to the original electrode. It should be noted that the contribution to the

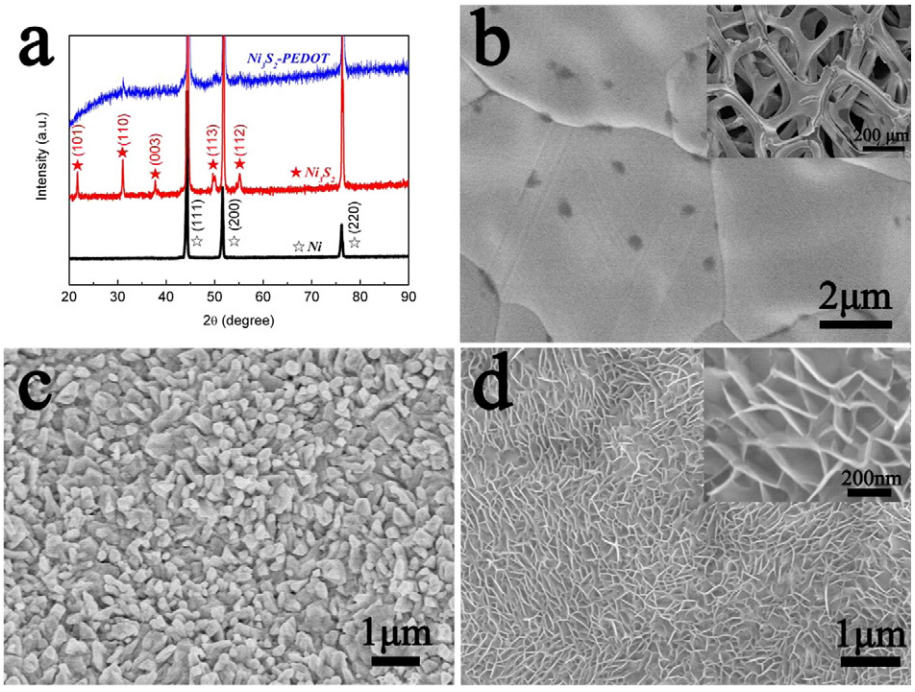

Fig. 1. (a) XRD patterns of Ni foam, Ni_3S_2 and Ni_3S_2-PEDOT. (b) Typical SEM image of Ni foam substrate. (c) Typical SEM image of Ni_3S_2 obtained from hydrothermal treatment on Ni substrate. (d) Typical SEM image of Ni_3S_2-PEDOT synthesized by electrodeposition of PEDOT on Ni_3S_2.

Table 1
Elemental composition of Ni_3S_2 and Ni_3S_2-PEDOT electrodes obtained by EDX analysis.

Electrode	O at%	S at%	Ni at%
Ni_3S_2	–	3.2 ± 0.2	96.8 ± 0.2
Ni_3S_2-PEDOT	9.7 ± 0.2	8.1 ± 0.2	82.2 ± 0.2

capacity between 2 and 2.8 V is not negligible. The initial charge capacity by cycling between 0.5 and 2 V is only 318.3 mAh g^{-1} with an irreversible capacity of 140 mAh g^{-1} and a capacity of 280 mAh g^{-1} after 30 cycles (Fig. 2f). As illustrated in Fig. 2c, the Ni_3S_2-PEDOT electrodes retain over 50% of the initial discharge specific capacity after 50 cycles, while Ni_3S_2 electrodes decay to only 6% of the initial discharge specific capacity. Fig. 2d displays that the monolithic Ni_3S_2-PEDOT electrode exhibits a reversible specific capacity of 600, 503, 408 and 310 mAh g^{-1} at a current density of 150, 300, 600 and 1200 mA g^{-1}, respectively. Particularly, when the current density decreased to 600 mA g^{-1} after rate cycles, the specific capacity of monolithic Ni_3S_2-PEDOT electrode recovers to 400 mAh g^{-1}, indicating a strong potential for rapid Na^+ insertion and extraction.

The cycle performance of Ni_3S_2 is so poor that the capacity retention is only 6% as demonstrated in Fig. 2c. As a consequence of Na^+ insertion/deinsertion during cycling, Ni_3S_2 typically breaks into Ni because it can react with Na to form Na_2S, leading to large volume expansion and destruction of structure, resulting in severe loss of capacity upon cycling. Stabilizing the interface between Ni_3S_2 and the electrolyte is therefore essential in improving the cycling performance. The ideal protective layer for Ni_3S_2 electrode needs to be chemically stable and mechanically strong. High flexibility is also desired to accommodate the volume expansion of Na^+ insertion/deinsertion without structure damage.

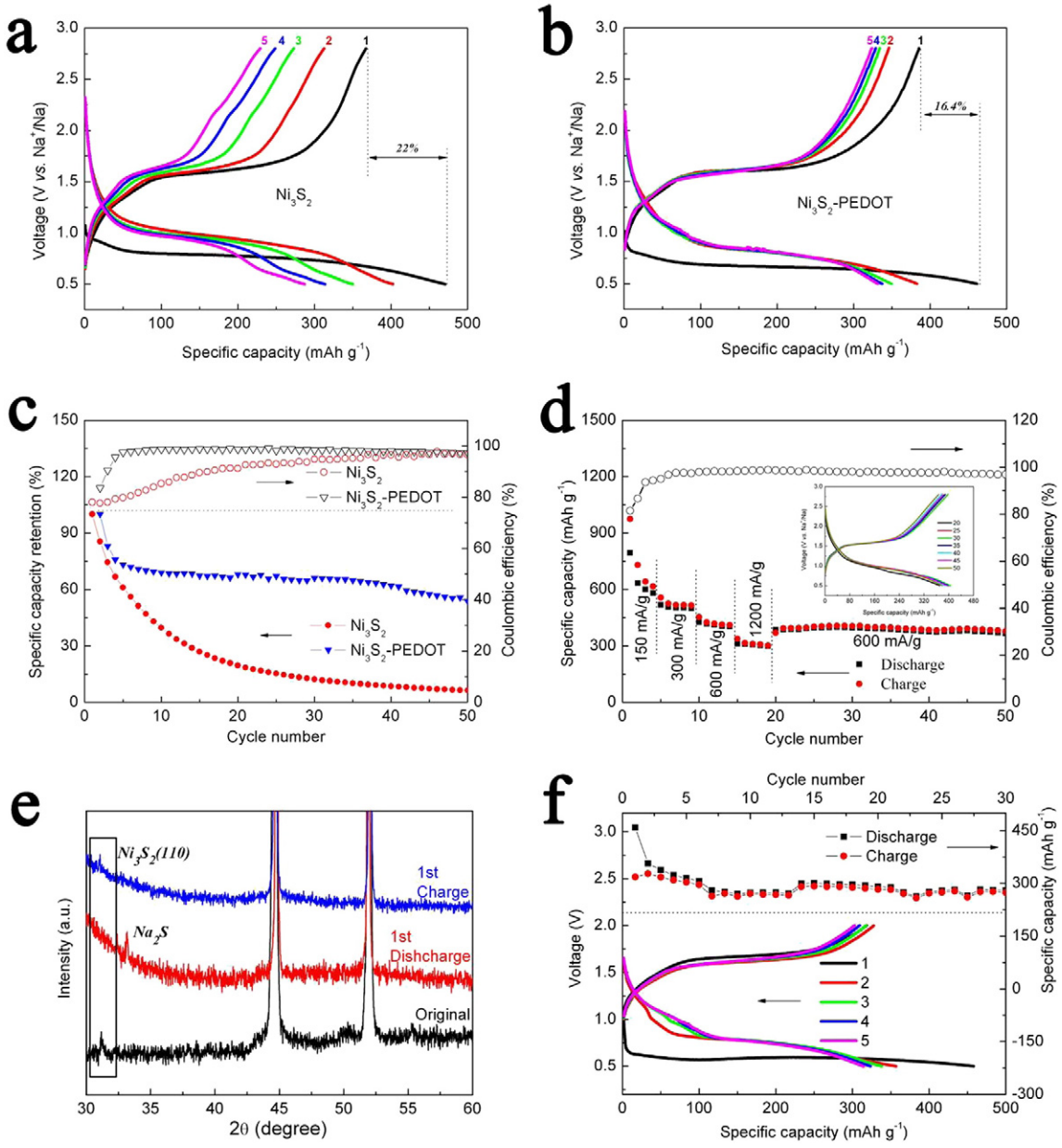

Fig. 2. The initial five charge–discharge profiles of Ni_3S_2 (a) and Ni_3S_2-PEDOT (b) electrodes, respectively. (c) The long-term cycling performance of Ni_3S_2 and Ni_3S_2-PEDOT electrodes. (d) The cycling and rate capabilities of monolithic Ni_3S_2-PEDOT electrode at various current densities from 150 to 1200 mA g^{-1}, as well as the galvanostatic charge–discharge profiles at a current density of 600 mA g^{-1} (inset). (e) XRD patterns of Ni_3S_2-PEDOT electrode: original, after 1st discharge and after 1st charge, respectively. (f) The initial five charge–discharge profiles of Ni_3S_2-PEDOT electrodes with a cut-off voltage of 2 V, as well as its long-term cycling performance.

The monolithic Ni_3S_2-PEDOT electrode delivers stable performance during cycling without any overcharging behavior, which further indicates the effective protection of PEDOT layer.

Here, we describe a flexible PEDOT coating with the aim of realizing cycle stability. The superior reversibility capacity of monolithic Ni_3S_2-PEDOT electrodes could be ascribed as follows: (i) Ni_3S_2 particles are directly grown on Ni foam, which improve the electrical contact between Ni_3S_2 active materials and Ni foam current collector. (ii) There is enough void space between the particles, which is beneficial to the contact of active materials and electrolyte. (iii) Monolithic design avoids the use of conductive additives and polymer binder and enhances the utilization of active materials. (iv) Ultrathin flexible PEDOT would encapsulate Ni_3S_2 inside the polymer shells with a buffer void, which maintains the structural integrity of Ni_3S_2 during charge–discharge process. All the desired functions of each component are efficiently utilized to realize a synergistic effect that monolithic Ni_3S_2-PEDOT electrodes exhibit desirable cycling stability for sodium-ion batteries.

4. Conclusions

In summary, a facile strategy has been developed to construct Ni_3S_2-PEDOT monolithic electrodes with stable electrochemical performance for sodium-ion batteries. The PEDOT layer would efficiently protect the Ni_3S_2 arrays from being wrecked by the severe volume change during charge–discharge process. The as-prepared Ni_3S_2-PEDOT electrodes display a reversible specific capacity of 400 mAh g^{-1} even at 600 mA g^{-1} and high initial coulombic efficiency (83.6%). This monolithic design of electrodes presented here will be further investigated for the extension to fabricating other new types of materials in sodium-ion batteries.

Conflict of interest

The authors declare no competing financial interest.

Acknowledgments

This work was supported by the National Natural Science Foundation of China (21271180), the China Postdoctoral Science Foundation (2014M561976), the National Program on Key Basic Research Project of China (973 Program) (No. MOST2011CB935700), the Key Technology Research Projects of Qingdao (No. 13-4-1-10-gx), and the Qingdao Key Lab of Solar Energy Utilization and Energy Storage Technology.

References

[1] M.D. Slater, D. Kim, E. Lee, C.S. Johnson, Sodium-ion batteries, Adv. Funct. Mater. 23 (2013) 947–958.
[2] Y. Kim, K.H. Ha, S.M. Oh, K.T. Lee, High-capacity anode materials for sodium-ion batteries, Chem. Eur. J. 20 (2014) 11980–11992.
[3] C. Zhu, K. Song, P.A. van Aken, J. Maier, Y. Yu, Carbon-coated $Na_3V_2(PO_4)_3$ embedded in porous carbon matrix: an ultrafast Na-storage cathode with the potential of outperforming Li cathodes, Nano Lett. 14 (2014) 2175–2180.
[4] Y. You, X.-L. Wu, Y.-X. Yin, Y.-G. Guo, High-quality Prussian blue crystals as superior cathode materials for room-temperature sodium-ion batteries, Energy Environ. Sci. 7 (2014) 1643–1647.
[5] R. Zhao, L. Zhu, Y. Cao, X. Ai, H.X. Yang, An aniline–nitroaniline copolymer as a high capacity cathode for Na-ion batteries, Electrochem. Commun. 21 (2012) 36–38.
[6] L. Xiao, Y. Cao, J. Xiao, W. Wang, L. Kovarik, Z. Nie, J. Liu, High capacity, reversible alloying reactions in SnSb/C nanocomposites for Na-ion battery applications, Chem. Commun. 48 (2012) 3321–3323.
[7] L. Fei, Y. Jiang, Y. Xu, G. Chen, Y. Li, X. Xu, S. Deng, H. Luo, A novel solvent-free thermal reaction of ferrocene and sulfur for one-step synthesis of iron sulfide and carbon nanocomposites and their electrochemical performance, J. Power Sources 265 (2014) 1–5.
[8] X. Rui, H. Tan, Q. Yan, Nanostructured metal sulfides for energy storage, Nanoscale 6 (2014) 9889–9924.
[9] J.-S. Kim, S.-W. Lee, X. Liu, G.-B. Cho, K.-W. Kim, I.-S. Ahn, J.-H. Ahn, G. Wang, H.-J. Ahn, Electrochemical properties of Na/Ni_3S_2 cells with liquid electrolytes using various sodium salts, Curr. Appl. Phys. 11 (2011) S11–S14.
[10] J.-S. Kim, H.-J. Ahn, H.-S. Ryu, D.-J. Kim, G.-B. Cho, K.-W. Kim, T.-H. Nam, J.H. Ahn, The discharge properties of Na/Ni_3S_2 cell at ambient temperature, J. Power Sources 178 (2008) 852–856.
[11] H.-S. Ryu, J.-S. Kim, J. Park, J.-Y. Park, G.-B. Cho, X. Liu, I.-S. Ahn, K.-W. Kim, J.-H. Ahn, J.-P. Ahn, S.W. Martin, G. Wang, H.-J. Ahn, Degradation mechanism of room temperature Na/Ni_3S_2 cells using Ni_3S_2 electrodes prepared by mechanical alloying, J. Power Sources 244 (2013) 764–770.
[12] D. Li, X. Li, X. Hou, X. Sun, B. Liu, D. He, Building a Ni_3S_2 nanotube array and investigating its application as an electrode for lithium ion batteries, Chem. Commun. 50 (2014) 9361–9364.
[13] J.-S. Kim, G.-B. Cho, K.-W. Kim, J.-H. Ahn, G. Wang, H.-J. Ahn, The addition of iron to Ni_3S_2 electrode for sodium secondary battery, Curr. Appl. Phys. 11 (2011) S215–S218.
[14] J. Yang, W. Guo, D. Li, C. Wei, H. Fan, L. Wu, W. Zheng, Synthesis and electrochemical performances of novel hierarchical flower-like nickel sulfide with tunable number of composed nanoplates, J. Power Sources 268 (2014) 113–120.
[15] J. Wang, D. Chao, J. Liu, L. Li, L. Lai, J. Lin, Z. Shen, Ni_3S_2@MoS_2 core/shell nanorod arrays on Ni foam for high-performance electrochemical energy storage, Nano Energy 7 (2014) 151–160.
[16] J. Jiang, Y. Li, J. Liu, X. Huang, C. Yuan, X.W. Lou, Recent advances in metal oxide-based electrode architecture design for electrochemical energy storage, Adv. Mater. 24 (2012) 5166–5180.
[17] C. Yuan, J. Li, L. Hou, X. Zhang, L. Shen, X.W.D. Lou, Ultrathin mesoporous $NiCo_2O_4$ nanosheets supported on Ni foam as advanced electrodes for supercapacitors, Adv. Funct. Mater. 22 (2012) 4592–4597.
[18] L. Yu, G. Zhang, C. Yuan, X.W. Lou, Hierarchical $NiCo_2O_4$@MnO_2 core–shell heterostructured nanowire arrays on Ni foam as high-performance supercapacitor electrodes, Chem. Commun. 49 (2013) 137–139.
[19] J. Qian, Y. Xiong, Y. Cao, X. Ai, H. Yang, Synergistic Na-storage reactions in Sn_4P_3 as a high-capacity, cycle-stable anode of Na-ion batteries, Nano Lett. 14 (2014) 1865–1869.
[20] R. Liu, S.B. Lee, MnO_2/Poly(3,4-ethylenedioxythiophene) coaxial nanowires by one-step coelectrodeposition for electrochemical energy storage, J. Am. Chem. Soc. 130 (2008) 2942–2943.
[21] X.Y. Zhang, J.S. Lee, G.S. Lee, D.K. Cha, M.J. Kim, D.J. Yang, S.K. Manohar, Chemical synthesis of PEDOT nanotubes, Macromolecules 39 (2006) 470–472.
[22] M. Culebras, C.M. Gómez, A. Cantarero, Enhanced thermoelectric performance of PEDOT with different counter-ions optimized by chemical reduction, J. Mater. Chem. A 2 (2014) 10109–10115.